The contribution of nitrogen deposition to the photosynthetic capacity of forests

K. Fleischer,[1] K. T. Rebel,[2] M. K. van der Molen,[3] J. W. Erisman,[1,4] M. J. Wassen,[5] E. E. van Loon,[6] L. Montagnani,[7,12] C. M. Gough,[8] M. Herbst,[9] I. A. Janssens,[10] D. Gianelle,[11] and A. J. Dolman[1]

Received 9 December 2011; revised 27 November 2012; accepted 27 January 2013; published 28 February 2013.

[1] Global terrestrial carbon (C) sequestration has increased over the last few decades. The drivers of carbon sequestration, the geographical spread and magnitude of this sink are however hotly debated. Photosynthesis determines the total C uptake of terrestrial ecosystems and is a major flux of the global C balance. We contribute to the discussion on enhanced C sequestration by analyzing the influence of nitrogen (N) deposition on photosynthetic capacity (A_{max}) of forest canopies. Eddy covariance measurements of net exchange of carbon provide estimates of gross primary production, from which A_{max} is derived with a novel approach. Canopy A_{max} is combined with modeled N deposition, environmental variables and stand characteristics to study the relative effects on A_{max} for a unique global data set of 80 forest FLUXNET sites. Canopy A_{max} relates positively to N deposition for evergreen needleleaf forests below an observed critical load of ~ 8 kg N ha^{-1} yr^{-1}, with a slope of 2.0 ± 0.4 (S.E.) μmol CO_2 m^{-2} s^{-1} per 1 kg N ha^{-1} yr^{-1}. Above this threshold canopy A_{max} levels off, exhibiting a saturating response in line with the N saturation hypothesis. Climate effects on canopy A_{max} cannot be separated from the effect of N deposition due to considerable covariation. For deciduous broadleaf forests and forests in the temperate (-continental) climate zones, the analysis shows the N deposition effect to be either small or absent. Leaf area index and foliar N concentration are positively but weakly related to A_{max}. We conclude that flux tower measurements of C fluxes provide valuable data to study physiological processes at the canopy scale. Future efforts need to be directed toward standardizing measures N cycling and pools within C monitoring networks to gain a better understanding of C and N interactions, and to disentangle the role of climate and N deposition in forest ecosystems.

Citation: Fleischer, K., K. T. Rebel, M. K. van der Molen, J. W. Erisman, M. J. Wassen, E. E. van Loon, L. Montagnani, C. M. Gough, M. Herbst, I. A. Janssens, D. Gianelle, and A. J. Dolman (2013), The contribution of nitrogen deposition to the photosynthetic capacity of forests, *Global Biogeochem. Cycles*, *27*, 187–199, doi:10.1002/gbc.20026.

1. Introduction

[2] The terrestrial biosphere is a major sink of atmospheric carbon (C), which is estimated to take up currently approximately 30% of anthropogenic produced carbon dioxide (CO_2) annually [*Schulze*, 2006; *Canadell et al*., 2007]. The strength of this land carbon sink has a high year-to-year variability, and due to major gaps in our understanding

All supporting information may be found in the online version of this article.

[1]Department of Earth Sciences, Cluster Earth and Climate, Vrije Universiteit Amsterdam, Amsterdam, The Netherlands.
[2]Environmental Sciences Group, Copernicus Institute of Sustainable Development, Faculty of Geosciences, Utrecht University, Utrecht, The Netherlands.
[3]Meteorology and Air Quality Group, Wageningen University and Research Centre, Wageningen, The Netherlands.
[4]Louis Bolk Institute, Driebergen, The Netherlands.
[5]Environmental Sciences Group, Copernicus Institute of Sustainable Development, Faculty of Geosciences, Utrecht University, Utrecht, The Netherlands.
[6]Computational Geo-Ecology, Institute of Biodiversity and Ecosystem Dynamics, University of Amsterdam, Amsterdam, The Netherlands.
[7]Faculty of Science and Technology, Free University of Bozen, Bozen-Bolzano, Italy.
[8]Department of Biology, The College of Humanities & Sciences, Virginia Commonwealth University, Richmond, Virginia, USA.
[9]Department of Bioclimatology, Faculty of Forest Sciences and Forest Ecology, Georg-August-University Göttingen, Göttingen, Germany.
[10]Department of Biology, University of Antwerp, Wilrijk, Belgium.
[11]Sustainable Agro-ecosystems and Bioresources Department, IASMA, Research and Innovation Centre, Fondazione Edmund Mach, San Michele all'Adige, TN, Italy.
[12]Forest Services, Autonomous Province of Bolzano, Bozen-Bolzano, Italy.

Corresponding author: K. Fleischer, Department of Earth Sciences, Cluster Earth and Climate, Vrije Universiteit Amsterdam, De Boelelaan 1085, 1081 HV Amsterdam, The Netherlands. (k.fleischer@vu.nl)

0886-6236/13/10.1002/gbc.20026

of the main drivers involved, we face large uncertainties in regard to its magnitude and geographical spread [*Ciais et al*., 2010; *Le Quéré et al*., 2009; *Le Quéré*, 2010; *Pan et al*., 2011].

[3] Terrestrial carbon sequestration may be enhanced globally due to increased nitrogen (N) deposition (N fertilization effect). The magnitude of the terrestrial C sink is expected to depend on the synergistic effect of N deposition and other drivers involved in terrestrial C sequestration [*Schulze*, 2006]. Additionally, changes in the pattern of N deposition, in relation to the distribution of different ecosystem types, may impact the rate of C sequestration [*Churkina et al*., 2010; *Dentener et al*., 2006]. Intensive agriculture, industry, and traffic, as well as the effect of global warming on biogeochemical cycles, has caused an acceleration of the N cycle and a doubling of reactive N in circulation since preindustrial times [*Erisman et al*., 2008, 2011; *Galloway et al*., 2008]. Forests play a major role in the uptake of C yet their productivity is often N limited [*LeBauer and Treseder*, 2008; *Wang et al*., 2010]. Still, the relative contribution of N deposition to the strength of the terrestrial carbon sink remains uncertain [*Janssens et al*., 2003; *Reay et al*., 2008].

[4] Estimates of the fertilizing effect of N range from almost no effect to 160 kg carbon sequestered per kg of N added, with most studies ranging between 35 to 65 kg C/kg N (*Erisman et al*. [2011] reviewing *Nadelhoffer et al*. [1999], *Högberg* [2007], *Magnani et al*. [2007], *Sutton et al*. [2008], *de Vries et al*. [2008, 2009], *Liu and Greaver* [2009], *Butterbach-Bahl and Gundersen* [2011], but see also *Thomas et al*. [2010]). The different fertilizing rates may be attributed to the fact that the C uptake per unit of N depends on the fate of N within the ecosystem (e.g., wood, leaf production, litter production, or leaching) [*Janssens and Luyssaert*, 2009]. This in turn is dependent on the current N status of an ecosystem, i.e., the level of which ecosystem productivity is limited by N availability.

[5] The N-saturation hypothesis predicts a nonlinear response of C uptake upon N addition [*Aber et al*., 1989, 1998]. Initially, N limited forests will experience increased growth with the addition of N, increasing plant C uptake and foliar N concentrations. A critical threshold of N saturation is reached when N availability exceeds microbial and plant demands, causing plants to achieve maximum foliar N concentrations, with some leaching of N. Prolonged N availability eventually leads to substantial leaching, decreases growth, and damage to forests due to nutrient imbalances [*Aber et al*., 1998; *Erisman and de Vries*, 2000; *Galloway et al*., 2003]. These stages are referred to as the N-limited, the intermediate, and the N-saturated stage and describe the N status of an ecosystem [*Butterbach-Bahl and Gundersen*, 2011]. In the N-limited stage, N deposition can increase photosynthesis and C uptake through stimulating leaf production and/or enhancing levels and capacity of leaf photosynthetic enzymes [*Janssens and Luyssaert*, 2009].

[6] Photosynthesis is limited by light, water, temperature, CO_2, and nutrient availability. The maximum rate of photosynthesis (A_{max} or photosynthetic capacity) is defined as the light-saturated rate of photosynthesis under optimal environmental conditions [*Field and Mooney*, 1986]. Plants adapt to their environment and invest N in photosynthetic enzymes, depending on the expected carbon return. A_{max} reflects the limitation of the environmental conditions, as well as physiological differences among species [*Schulze et al*., 2005]. Therefore, A_{max} is an integral measure of the combined biochemical and physical limitations of photosynthesis, set by genetic and environmental constraints over various time-scales [*Field and Mooney*, 1986; *Schulze*, 2006]. At the leaf level, photosynthesis-climate and photosynthesis-nitrogen relationships have been well established at managed greenhouse or field experiments. Temperature and water availability affect leaf level photosynthesis positively with varying optima [*Jarvis*, 1976; *Schulze et al*., 2005], and foliar N concentration is positively and linearly related to A_{max} across a large variety of plant species and scales [*Field and Mooney*, 1986; *Schulze*, 2006].

[7] Translating leaf level photosynthesis to canopy scale remains challenging. The driving factors of photosynthesis at the canopy scale may be obscured, because assimilation rates are further influenced by canopy structure and physiological functioning [*Baldocchi et al*., 2002]. However, mean annual temperature and precipitation are often found to be positively related to canopy photosynthesis [*Luyssaert et al*., 2007; *Reichstein et al*., 2007; *Kergoat et al*., 2008; *Groenendijk et al*., 2009]. Furthermore, leaf area index (LAI) and foliar N concentrations have been suggested to be the principal factor when translating leaf to canopy photosynthesis [*Schulze*, 2006; *Kergoat et al*., 2008; *Lindroth et al*., 2008; *Ollinger et al*., 2008; *Dronova et al*., 2011]. However, LAI and foliar N are not independent of N deposition or climate, because they relate to both N availability and climate conditions [*Bequet et al*., 2011; *Kergoat et al*., 2008; *De Vries et al*., 2003].

[8] Nitrogen availability is believed to increase canopy photosynthetic capacity (1) by increasing photosynthetic enzyme availability and hence higher leaf A_{max}, and/or (2) by an increase in leaf area and leaf production increasing canopy A_{max}. The relative importance of the two mechanisms remains uncertain [*Janssens and Luyssaert*, 2009].

[9] Understanding and testing the enhancing effect of N deposition on photosynthesis is one key area of needed research to decrease the uncertainty in the overall effect of N deposition on C sequestration [*Janssens and Luyssaert*, 2009]. However, to our knowledge, the relationship between N deposition and canopy photosynthesis has not been tested through direct observations across a range of forest conditions. Our approach focuses on a more mechanistic assessment of controls on photosynthesis, employing A_{max} derived from half-hourly measurements of gross primary production (GPP), whereas most studies of canopy photosynthesis have focused on some integrated measure of GPP. We are aware that climate interactions, i.e., the high correlation between climate and N deposition, have complicated previous assessments of a pure N deposition effect on C sequestration in other observational spatial data sets [*Piao et al*., 2009; *Sutton et al*., 2008; *Aber et al*., 2003]. Notably, our study tests the suitability of the FLUXNET network [*Baldocchi et al*., 2001] in resolving these confounding factors between drivers of the C balance, which remains unexplored and deserves critical attention.

[10] In this study we attempt to quantify the relationship between N deposition and canopy A_{max} of forest ecosystems across the globe. Additionally, we want to establish whether the relationships between N deposition and A_{max} differ between climate zones and forest types, and to which degree N deposition and canopy A_{max} are connected to climatic drivers. All of which is relevant for estimating the enhancing effect of N deposition on photosynthesis on a global scale. We achieve this by testing the relative influence of the potential main drivers on canopy photosynthetic capacity, and their interactions, for 73 forest sites around the globe. Specifically, we test the following three hypotheses:

[11] 1. Canopy A_{max} varies across forest sites depending on the limitations set by genetic and environmental conditions, i.e., physiology, water, temperature and nutrition. We hypothesize that N deposition explains additional variation in A_{max} beyond that explained by climate alone.

[12] 2. We hypothesize that the relationship between N deposition and canopy A_{max} is nonlinear. The relationship is positive and linear at low N deposition rates (~ 0–15 kg N $ha^{-1}\,yr^{-1}$), approaching a maximum at critical N loads, and exhibiting a neutral or negative trend with increasing N deposition.

[13] 3. Additionally to the constraints above, we expect that canopy A_{max} is influenced by LAI and foliar N concentration. We hypothesize that LAI and/or foliar N are positively related to A_{max} and in turn, foliar N and LAI are expected to be related to N deposition.

[14] To test our hypotheses, we used the FLUXNET database to calculate canopy A_{max} based on half-hourly flux measurements, combined these with modeled N deposition maps and stand characteristics, and conducted regression and other statistical analysis on the resulting data set.

2. Data and Methods

2.1. Carbon Flux and Nitrogen Deposition Data

[15] A data set, composed of half-hourly measurements of net ecosystem exchange (NEE) of carbon, based on the eddy-covariance technique, was compiled for a large number of forest FLUXNET sites (La Thuile) from 1998 to 2005 inclusive [*Baldocchi et al*., 2001]. The latitudinal range of these sites is 68.4°N to 35.7°S, with the majority of them located in Europe and the northeastern United States (Figure 1). The forest types are classified according to the International Geosphere-Biosphere Program (IGBP)-vegetation classification and cover the following forest types: evergreen needleleaf, evergreen broadleaf, deciduous broadleaf, and mixed forest [*Loveland et al*., 2000]. The sites cover the major climate zones of the world: boreal, temperate, temperate-continental, subtropical-Mediterranean, and tropical, which are classified according to the Köppen-Geiger climate classification [*Kottek et al*., 2006].

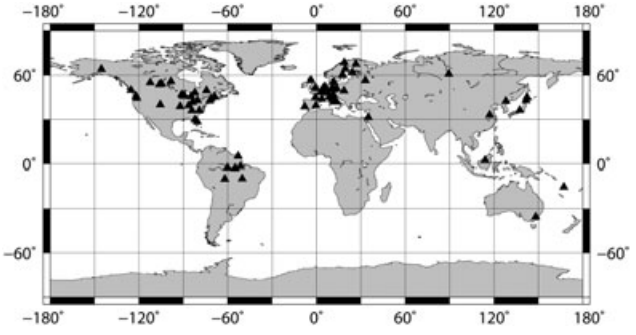

Figure 1. The geographical distribution of the 80 FLUXNET forest sites (solid triangle).

[16] Recently disturbed sites and years with less than 12,000 half-hourly data points were excluded from the analyses to avoid unrepresentative data years (a complete year contains a time-series of 17,520 half-hourly data points), resulting in a data set that collectively represents 317 years of measured CO_2 fluxes from 80 managed and unmanaged forest sites.

[17] Estimates of total N deposition (Ndepo) for each site were taken from an ensemble calculation of global deposition models for the year 2000 available at a resolution of 1° × 1° [*Dentener et al*., 2006] and were used to compare to the flux measurements. Total N from these models represents the estimated total deposition for reduced and oxidized reactive N from dry and wet deposition. FLUXNET tower footprints vary with topography and wind conditions but are approximately 1 km^2 [*Baldocchi et al*., 2001], considerably smaller than the resolution of the modeled N deposition.

2.2. Calculation of Canopy A_{max}

[18] Flux towers measure both NEE and photosynthetic photon flux density (PPFD) at the canopy scale as 30 min averages. GPP estimates were obtained from the data set and are derived from NEE following the flux partitioning method described by *Reichstein et al*. [2005]. GPP is defined positive and NEE, as well as ecosystem respiration (R_{eco}), follow the classical micrometeorological conventions, being positive for upward CO_2-fluxes: $GPP = -NEE + R_{eco}$. Information on harmonized data-processing procedures with associated errors can be found in *Papale et al*. [2006]. Uncertainty in GPP estimates due to the flux partitioning method is expected to be low [*Desai et al*., 2008].

[19] Canopy A_{max} was estimated by using light response curves, setting out GPP against PPFD and by taking the average of the upper 95th–98th percentile of GPP values in the light-saturated zone. Per site, all available data (spanning multiple years) were combined to derive a single light response curve and hence a single estimate of A_{max}. Therefore, the estimates represent the most optimal conditions observed at each site for the selected research period, 1998–2005. Details on the establishment of light-saturation and examples of light response curves and derived A_{max} values of representative sites can be found in Appendix A.

2.3. Environmental and Ecological Variables

[20] Annual precipitation (Precip), mean annual temperature (MAT), and two additional temperature indices were calculated based on the half-hourly measurements taken at the flux towers. The temperature indices are mean temperature of the realized optimum (MTO) and mean temperature deviation from the realized optimum (MTD). MTO is the mean of temperature values corresponding to the time of the CO_2 fluxes of A_{max}, reflecting the temperature of the most optimal conditions for each site. MTD is defined as the absolute mean deviation from MTO for the whole year. It represents a measure of how close the annual temperature

is to the temperature at which A_{max} is reached. MTD is tested as an alternative index for MAT in the regression analysis, because MAT is not expected to have a direct ecological link to photosynthesis [*Kergoat et al*., 2008]. Both temperature indices and precipitation were calculated per year and averaged per site, producing one average per site. Precipitation measurements were not available for three sites, which were excluded from all regression analyses (Table A1).

[21] Data on LAI (in $m^2 m^{-2}$) ($n = 72$) and foliar N concentration on percent mass basis (g N/g dry weight) ($n = 39$) were derived for each site from the literature or through personal communication with the principal investigators of the sites. If available, the seasonal maximum for tree LAI and the foliar N concentration for the growing season were used, corresponding to the time at which optimal growth conditions are expected. For both, data in close agreement to the flux measurement years were selected. A complete list of FLUXNET site information, including site ID, name, latitude, forest type, climate zone, modeled N deposition, estimates of A_{max}, foliar N concentrations, and LAI used in this analysis, and also site citations and citations for foliar N and LAI can be found in the supporting information (Table A1).

2.4. Regression Analysis

[22] Multiple linear and nonlinear regression models were built to analyze the influence of N deposition, temperature, precipitation, LAI, and foliar N on canopy A_{max} for the different forest types and climates. Models were built with increasing complexity. All univariate linear effects on A_{max} were tested before applying a forward step selection for the best multivariate model. The Michaelis-Menten function was chosen for the nonlinear estimate of the A_{max} response to N deposition. Model parameters were estimated using a least squares criterion. Model accuracy was compared using different statistics: the adjusted coefficient of determination (adj. R^2), the Akaike information criterion (AIC) and the root-mean-square error (RMSE) [*Hilborn and Mangel*, 1997; *Burnham and Anderson*, 1998]. Linear correlations between predictors were assessed with the Pearson correlation coefficient (PCC) [*Rodgers and Nicewander*, 1988]. Power analysis was performed for selected groups to assess whether the absence of statistical significance is due to insufficient sample size [*Cohen*, 1988; *Kravchenko and Robertson*, 2011] (Appendix B). Four sites had unusually high leverage on model results and were excluded from the analysis to avoid biased results (Table A1). The exclusion of these sites and sites with missing precipitation data yielded an effective data set of 73 sites for the regression analysis (Table 1). The analyses were conducted in R [*R Development Core Team*, 2011]. The slopes of the model parameter for N deposition are estimates for the potential N deposition effect on photosynthesis, allowing extrapolation to an N effect on C sequestration via increases in photosynthesis. The calculation of C sequestration per unit N deposition is detailed in Appendix C.

Table 1. Overview of Available Forest Sites Separated by Forest Types (Rows) and Climate Zones (Columns); Forest Types Abbreviations Are Deciduous Broadleaf (DBF), Evergreen Broadleaf (EBF), Evergreen Needleleaf (ENF) and Mixed Forest (MF), Climate Zone Abbreviations Are Temperate (TE), Tropical (TR), Subtropical-Mediterranean (SM), Arctic (AR), Boreal (BO), Temperate-Continental (TC), and Dry (DR)

	AR	BO	DR	SM	TC	TE	TR	Total
DBF	0	1	0	7	6	5	0	19
EBF	0	0	0	3	0	1	9	13
ENF	0	11	1	6	5	9	0	32
MF	0	1	0	0	6	2	0	9
Total	0	13	1	16	17	17	9	73

3. Results

[23] The 73 forest sites from the FLUXNET database included in the regression analysis cover a modeled N deposition range from ~0 to 32 kg N $ha^{-1} yr^{-1}$. The data set is dominated by evergreen needleleaf forests (ENF) and deciduous broadleaf forests (DBF), with 32 and 19 sites, respectively. These sites are predominately found in the boreal, temperate, temperate-continental, and subtropical-Mediterranean climate zones (Table 1 and Figure 1). The results focus primarily on evergreen needleleaf and deciduous broadleaf forests. In order to quantify the relationship between A_{max} and Ndepo, the variation of A_{max} in comparison to the most important climate variables MAT, MTO, MTD, and Precip (3.1.) and with Ndepo (3.2.) individually is shown first. Subsequently, multivariate regression models are built to quantify the relative contribution of each of the predictor variables and assess correlations among predictors (3.3.). Subsets of the data are analyzed to reflect the N limited range or sites of the same climate zones. For Ndepo either a linear or the Michaelis-Menten function is selected. Finally, the influence of LAI and foliar N on A_{max} and their relationship with Ndepo is assessed (3.4.). The main regression results are detailed (Table 2) and the correlations of Ndepo with the environmental variables are shown for evergreen needleleaf forests (Table 3). For clarity only the main findings and statistically significant results are shown.

3.1. Climate Effects on A_{max}

[24] Evergreen needleleaf and deciduous broadleaf forests are characterized by distinct patterns of the photosynthesis-climate comparisons, and show little overlap. MTO is not related to A_{max} for the individual forest types but differs statistically between evergreen needleleaf (sample mean ± 1SD: $MTO_{ENF} = 18.6 \pm 3.6°C$) and deciduous broadleaf forests (sample mean ± 1SD: $MTO_{DBF} = 22.3 \pm 3.9°C$) (Figure 2a). Along the range of MTD, both forest types show a negative trend (Figure 2b) indicating that photosynthetic capacity is larger if the temperature is generally closer to the optimum. Mean values of MTD are not different for deciduous broadleaf (sample mean ± 1SD: $MTD_{DBF} = 12.9 \pm 2.9°C$) and evergreen needleleaf forests (sample mean ± 1SD: $MTD_{ENF} = 12.2 \pm 4.0°C$); the latter occupying a somewhat larger range. MAT is positively related to A_{max} for evergreen needleleaf forests, however, only weakly ($R^2 = 0.11$) because not all sites follow the general trend (Figure 2c and Table 2, subset 1). Precip and MTD show a stronger relationship with A_{max} ($R^2 = 0.47$ and 0.28, respectively) for evergreen needleleaf forests (Figure 2d and Table 2, subset 1). For deciduous broadleaf forests however the relationships between A_{max} and Precip, MAT or MTD are

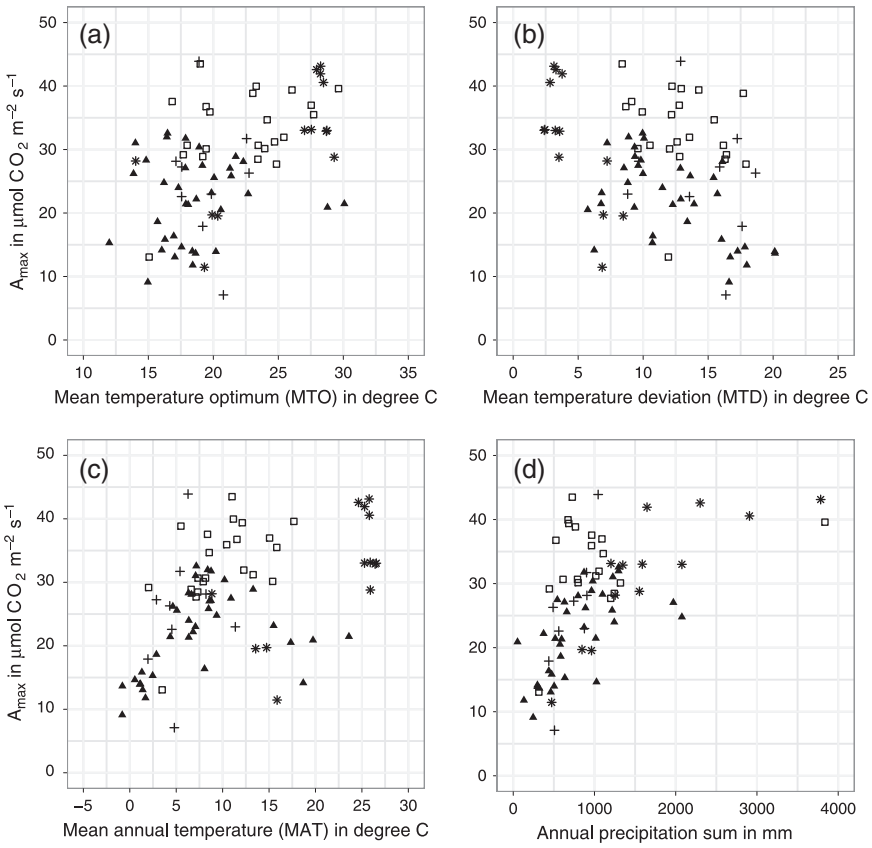

Figure 2. Maximum rates of photosynthesis (A_{max}) against climate variables ($n = 80$): (a) mean temperature of A_{max} measurements (MTO in °C), (b) mean deviation from temperature optimum (MTD in °C), (c) mean annual temperature (MAT in °C), and (d) annual precipitation (precipitation in mm) ($n = 77$). Symbols represent different forest types; deciduous broadleaf (DBF, open square), evergreen broadleaf (EBF, asterisk), evergreen needleleaf (ENF, solid triangle), and mixed forest (MF, plus).

not significant after the exclusion of the arctic forest site with a very low A_{max} (Figures 2b, 2c, and 2d, Table A1, regression not shown).

[25] For evergreen broadleaf forests, there is a strong positive relationship to Precip ($R^2 = 0.62$, $p < 10^{-3}$, $n = 13$) and a weaker one to MAT ($R^2 = 0.44$, $p = 0.008$, $n = 13$). MTD explains more variation in A_{max} for evergreen broadleaf forests ($R^2 = 0.56$, $p = 0.002$, $n = 13$) than MAT.

3.2. N Deposition and A_{max}

[26] A_{max} estimates for all forest sites follow a general positive trend with increasing N deposition (Figure 3a and 3b) but responses differ between forest types and climates. For evergreen needleleaf forests, the relationship between A_{max} and N deposition exhibits a nonlinear, saturating response (Figure 3a). The initial linear increase in A_{max} at low N deposition rates levels off at N deposition rates of ~ 10 kg N ha^{-1} yr^{-1} (Figure 3a). The nonlinear estimation of the N deposition response of A_{max} gives the best fit for all evergreen needleleaf forests (Table 2, subset 1). The piecewise regression of A_{max} versus N deposition, employed to derive the best breakpoint for two linear intervals, derives a breakpoint at 8 ± 1.5 (S.E.) kg N ha^{-1} yr^{-1}. This threshold represents an estimate for the critical load of N deposition for evergreen needleleaf forests. Based on this assessment the N-limited range for subsequent analyses is defined for N deposition rates below 8 kg N ha^{-1} yr^{-1} (see section 3.3). The slope of the observed initial increase for sites in this N-limited range was 2.0 ± 0.4 µmol CO_2 m^{-2} s^{-1} per 1 kg N ha^{-1} yr^{-1} (Table 2, subset 2). This value represents the highest observed estimate of the Ndepo effect on A_{max} for evergreen needleleaf forests in the N-limited range.

[27] Deciduous broadleaf forests are in general characterized by higher A_{max} than evergreen needleleaf forests at similar rates of N deposition in our data set. However, a nonlinear or linear relationship is not significant for deciduous broadleaf forests and only indicative ($R^2 = 0.15$, $p = 0.057$, $n = 19$; Figure 3a). Power analysis reveals that the sample size for deciduous broadleaf forests is large enough to detect any relationship between A_{max} and Ndepo with an R^2 value greater than 0.32 with 80% probability (Appendix B). That means that given our sample size it can be inferred that the relationship is unlikely to equate to an R^2 of more than 0.32, hence is either small or absent. For mixed forests there is no visible trend along the axis of N deposition (Figure 3a). However, the low sample size of 9 mixed forest sites similarly does not allow inferring an absence of a relationship. Only a strong relationship with an R^2 value larger than 0.55 would be detected with nine samples (Appendix B). Evergreen broadleaf forests are negatively related to N deposition ($R^2 = 0.43$, $p = 0.009$, $n = 13$).

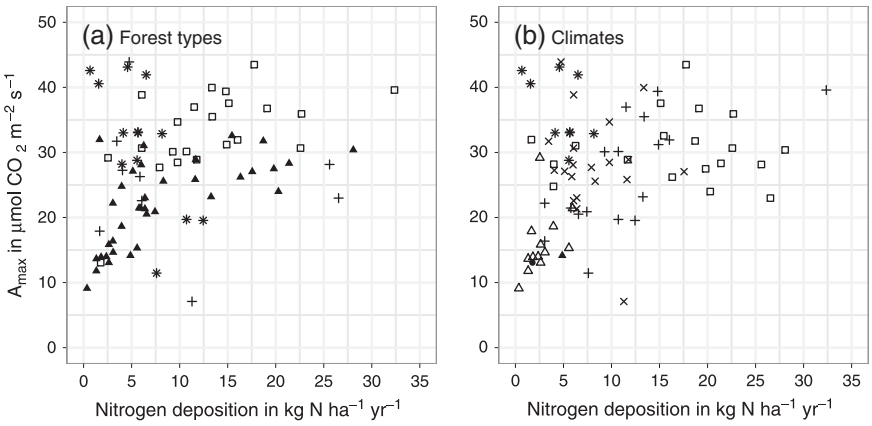

Figure 3. Maximum rates of photosynthesis (A_{max}) against N deposition ($n = 80$), marked with (a) different forest types on the left; deciduous broadleaf (DBF, open square), evergreen broadleaf (EBF, asterisk), evergreen needleleaf (ENF, solid triange) and mixed forest (MF, plus), and marked with (b) different climate zones on the right; arctic (solid circle), boreal (open triangle), dry (solid triangle), subtropical-Mediterranean (plus), temperate-continental (cross), temperate (open square), and tropical (asterisk).

[28] There is a clear clustering of sites when grouped for climate, e.g., boreal evergreen needleleaf forests are found at the low N deposition and A_{max} range, with a positive linear trend. In contrast, temperate-continental and temperate sites show no visible trend along the N deposition gradient, with the latter occupying the high end of the covered N deposition range (Figure 3b).

3.3. Nitrogen's Effect on A_{max} After Accounting for Climate

[29] The subsequent regression analysis focuses on evergreen needleleaf forests. The significant responses of A_{max} to the environmental predictors and Ndepo and sufficient data allow a detailed analysis of this forest type ($n = 32$). Regression models are built to assess the relative significance of climate (MAT, MTD, and Precip) and Ndepo in determining A_{max} for evergreen needleleaf forests. A brief section on evergreen broadleaf forests to clarify the relative importance of climate and Ndepo for this forest type is added.

[30] The nonlinear function of Ndepo is the best model for A_{max} for all evergreen needleleaf forests (Table 2, subset 1). Linear terms for MTD, Precip, and MAT are weaker predictors, as expressed by AIC and RMSE. Combining MTD with Ndepo derives the best linear model and explains slightly more variation in A_{max} than a pure climatic model with MTD and Precip (Table 2, subset 1). For sites in the N-limited range (Ndepo < 8 kg N ha^{-1} yr^{-1}, section 3.2.) the linear combination of Ndepo and Precip performs best, reducing the previously observed Ndepo effect to 1.7 ± 0.4 (S.E.) µmol CO_2 m^{-2} s^{-1} per 1 kg N ha^{-1} yr^{-1} (Table 2, subset 2).

[31] For all evergreen needleleaf sites, MAT is a weak predictor of A_{max} (e.g., Table 1, subset 1) because five evergreen needleleaf forest sites have relatively high mean average temperatures (>15°C) and form outliers on the otherwise linear relationship with A_{max} (Figure 2c). The sites belong to the subtropical-Mediterranean and dry climate zones and there are some indications that A_{max} may be soil moisture limited at these sites, although soil moisture data are only available for two of the five sites (not shown). They are therefore regarded as representatives of water-limited ecosystems and are excluded from further analyses. This causes the relationships of A_{max} with the temperature indices (MAT and MTD) and Precip to become considerably stronger compared to subset 1 (Table 2, subset 3). The pure climatic model of MAT and Precip best explains the variation in A_{max} for this subset, with an R^2 of 0.84. MAT as a single predictor explains a large part of the variation in A_{max} with an R^2 of 0.77, and a nonlinear model of Ndepo explains slightly less. It is, however, impossible to separate the effect of climate and Ndepo with certainty in this subset, because the linear correlations of Ndepo with Precip, MTD, and MAT are larger than ± 0.6 (Table 3), and Ndepo as a linear predictor of A_{max} results in an R^2 of 0.54 (Table 2, subset 3).

[32] Restricting the last subset further to the N-limited range (Ndepo < 8 kg N ha^{-1} yr^{-1}, section 3.1) selects 15 sites, of which 11 are boreal. Therefore, boreal sites are analyzed alone (Table 2, subset 4) resulting in MAT and Ndepo to have a similarly strong univariate relation to A_{max} ($R^2 = 0.64$ and 0.67, respectively). In this smaller subset, the correlations between climate variables and Ndepo are even stronger than in the previous subsets with a PCC of up to 0.85 for MAT and Ndepo (Table 3). The slope for the Ndepo effect on the boreal forests is 1.6 ± 0.3 (S.E.) µmol CO_2 m^{-2} s^{-1} per 1 kg N ha^{-1} yr^{-1}. This close connection of MAT and N deposition is remarkable, because 11 boreal evergreen needleleaf forests from Europe and North America are considered, moving across an axis of N deposition originating from two continents. Limited data are available within each climate zone (Table 1) and only univariate analyses can be undertaken. For evergreen needleleaf forests in the temperate, temperate-continental, or subtropical-Mediterranean zone alone, no significant relationships between A_{max} and Ndepo or climate emerge.

[33] For evergreen broadleaf forests, the best multivariate model is the combination of MTD and Precip ($R^2 = 0.74$, $p < 10^{-3}$, $n = 13$). The predictive power of the environmental variables is therefore stronger than the observed negative relationship with Ndepo for this forest type (see section 3.2.).

Table 2. Results of Regression Models for Evergreen Needleleaf Forests Describing A_{max} (in $\mu mol\,m^{-2}\,s^{-1}$) as a Function of N Deposition (Ndepo in $kg\,N\,ha^{-1}\,yr^{-1}$), Mean Temperature Deviation (MTD in °C), Mean Annual Temperature (MAT in °C), Annual Precipitation (Precip in mm) for Evergreen Needleleaf Forest Sites; Model Accuracy Is Reported With the Coefficient of Determination, Adjusted for the Number of Variables in the Model (adj. R^2), the Root Mean Square Error (RMSE), and the Akaike Information Criterion (AIC); Parameter Estimates With Standard Error Are Reported ($a1$, $a2$, and c or $a3$), p-value and/or Level of Significance of the Model (p), Results Are Separated for Four Subsets

Model	$a1$	$a2$	c or $a3$	adj. R^2	RMSE[a]	AIC[a]	p
Subset 1) Entire range of Ndepo and all climates ($n = 32$)							
$A_{max} \sim (a1 * Ndepo) / (Ndepo + a2)$	31.8 ± 1.9	2.5 ± 0.5	--	--	3.6	178.3	***
$A_{max} \sim (a1 * Ndepo) + (a2 * Precip) + c$	0.47 ± 0.1	0.008 ± 0.003	12.4 ± 1.6	0.624	3.9	185.8	$<10^{-6}$***
$A_{max} \sim (a1 * MTD) + (a2 * Precip) + c$	-0.55 ± 0.21	0.011 ± 0.003	20.6 ± 3.6	0.559	4.2	190.9	$<10^{-7}$***
$A_{max} \sim (a1 * Precip) + c$	0.014 ± 0.0025	--	12.3 ± 1.9	0.471	4.7	195.8	$<10^{-5}$***
$A_{max} \sim (a1 * MTD) + c$	-0.89 ± 0.25	--	32.4 ± 3.2	0.281	5.5	205.6	$<10^{-2}$**
$A_{max} \sim (a1 * MAT) + c$	0.39 ± 0.18	--	18.6 ± 1.7	0.107	6.1	212.6	0.0382*
Subset 2) N-limited range (Ndepo < 8) and all climates ($n = 21$)							
$A_{max} \sim (a1 * Ndepo) + (a2 * Precip) + c$	1.7 ± 0.4	0.006 ± 0.003	8.0 ± 2.0	0.599	3.4	118.4	$<10^{-3}$***
$A_{max} \sim (a1 * Ndepo) + c$	2.0 ± 0.4	--	10.0 ± 1.9	0.524	3.8	121.2	$<10^{-3}$***
$A_{max} \sim (a1 * MTD) + (a2 * Precip) + c$	-0.49 ± 0.22	0.009 ± 0.004	20.1 ± 4.0	0.410	4.1	126.5	$<10^{-2}$**
$A_{max} \sim (a1 * Precip) + c$	0.011 ± 0.004	--	12.4 ± 2.2	0.289	4.6	129.6	$<10^{-2}$**
$A_{max} \sim (a1 * MTD) + c$	-0.66 ± 0.24	--	26.9 ± 3.3	0.244	4.7	130.9	0.0133*
Subset 3) Entire Ndepo range, excluding subtropical-Mediterranean and dry climates ($n = 25$)							
$A_{max} \sim (a1 * MAT) + (a2 * Precip) + c$	1.3 ± 0.2	0.008 ± 0.002	10.1 ± 1.4	0.842	2.7	129.2	$<10^{-10}$***
$A_{max} \sim (a1 * MAT) + c$	1.7 ± 0.2	--	13.6 ± 1.2	0.766	3.4	138.2	$<10^{-9}$***
$A_{max} \sim (a1 * Ndepo) / (Ndepo + a2)$	32.7 ± 2.0	2.5 ± 0.6	--	--	3.5	139.1	***
$A_{max} \sim (a1 * MTD) + c$	-1.5 ± 0.2	--	42.3 ± 3.3	0.619	4.3	150.3	$<10^{-6}$***
$A_{max} \sim (a1 * Ndepo) + c$	0.7 ± 0.1	--	15.6 ± 1.5	0.542	4.8	154.9	$<10^{-5}$***
$A_{max} \sim (a1 * Precip) + c$	0.016 ± 0.003	--	10.2 ± 2.4	0.538	4.8	155.1	$<10^{-5}$***
Subset 4) N-limited range for boreal climates ($n = 11$)							
$A_{max} \sim (a1 * Ndepo) + c$	1.6 ± 0.3	--	10.2 ± 1.1	0.674	1.7	48.7	0.001**
$A_{max} \sim (a1 * MAT) + c$	1.8 ± 0.4	--	12.2 ± 0.8	0.638	1.8	49.9	0.002**

Significance codes: 0 "***" 0.001 "**" 0.01 "*" 0.05 "." 0.1 " " 1.

[a]For model accuracy measures AIC and RMSE: a smaller value represents a better fit for the model, AIC is only comparable for models in the same subset, a difference in AIC between two models of > 2 is regarded as significant.

Table 3. Pearson Correlation Coefficients (PCC) for N Deposition (Ndepo) With the Environmental Variables for the Four Subsets, PCC of >0.6 Are Strong Correlations and Printed in Bold Italics

	Precipitation (Precip)	Mean Temperature Deviation (MTD)	Mean Annual Temperature (MAT)
Subset 1	***0.61***	−0.48	0.29
Subset 2	0.39	***−0.75***	***0.68***
Subset 3	***0.64***	***−0.68***	***0.71***
Subset 4	0.55	***−0.78***	***0.85***

3.4. Mechanisms for the N-effect

[34] The influence of LAI and foliar N on A_{max} is assessed by separately relating Ndepo to LAI and foliar N, because Ndepo is expected to increase canopy photosynthesis via increased leaf production and/or foliar N concentrations. Sample sizes differ in regression analysis to figures due to excluded sites (see section 2.4). For clarity, regression results are not shown in Table 2.

[35] Foliar N is lower for evergreen needleleaf forests (sample mean ± 1SD: $folN_{ENF} = 1.07 \pm 0.27$ %N) than

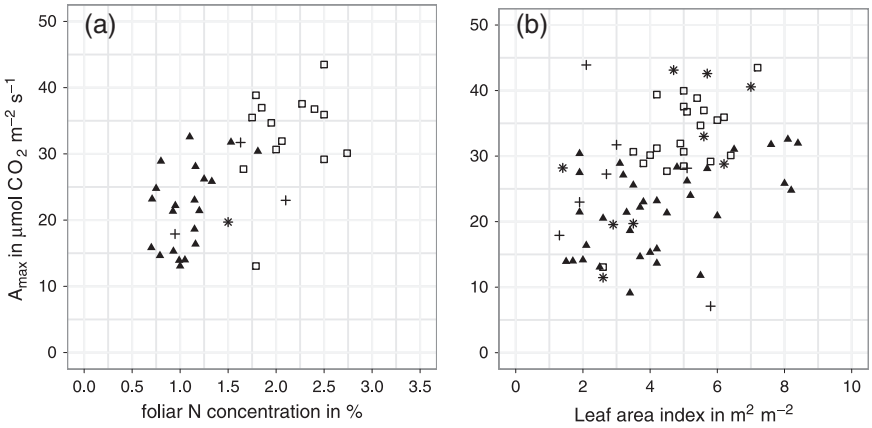

Figure 4. Maximum rates of photosynthesis (A_{max}) against biotic variables: (a) A_{max} against foliar N concentration (in %N per g dry weight) ($n = 39$) and (b) A_{max} against leaf area index (in $m^2\,m^{-2}$) ($n = 72$). Symbols represent different forest types; deciduous broadleaf (DBF, open square), evergreen broadleaf (EBF, asterisk), evergreen needleleaf (ENF, solid triangle), and mixed forest (MF, plus).

for deciduous broadleaf forests (sample mean ± 1SD: $folN_{DBF} = 2.13 \pm 0.35$ %N) (Figure 4a). As a result, the positive relationship between foliar N and A_{max} is significant across all forest sites ($R^2 = 0.53$, $p < 10^{-6}$, $n = 35$), while for the individual forest types it is small or absent (evergreen needleleaf forests: $R^2 = 0.22$, $p < 0.05$, $n = 19$; deciduous broadleaf forests: no significant relationship).

[36] Leaf area index is significantly and positively related to A_{max} across all forest types ($R^2 = 0.17$, $p < 10^{-3}$, $n = 66$, Figure 4b) and for the evergreen needleleaf forests ($R^2 = 0.18$, $p < 10^{-2}$, $n = 32$, Figure 4b). No relationships emerge for the other forest types. The explanatory power of LAI on variation in A_{max} is limited and not comparable to the explanatory power of the climate variables or N deposition.

[37] Ndepo shows no significant linear relationship with LAI for the evergreen needleleaf forests, whereas foliar N does ($R^2 = 0.41$, $p = 0.002$, $n = 19$). This strong positive relationship was not detectable within the N limited range, where the strongest influence is expected. The connection between foliar N and Ndepo is also significant across all forest sites ($R^2 = 0.22$, $p = 0.002$, $n = 35$) but weaker than within evergreen needleleaf forests.

4. Discussion

4.1. Estimates of the N Deposition Effect

[38] Our first hypothesis states that N deposition explains additional variation in canopy A_{max} beyond that of environmental variables. We demonstrate that N deposition and climate variables are significantly related to A_{max} for evergreen needleleaf forests. N deposition alone explains most variation of A_{max} when considering all evergreen needleleaf forests. Temperature and precipitation however explain most variation of A_{max} after the exclusion of water-limited forests. The water-limited sites cause the overall predictability of A_{max} by temperature and precipitation to decrease and a model with N deposition alone performs better than a pure climatic model.

[39] Splitting the forest sites into more meaningful subgroups shows that both N deposition and climate are significantly related to A_{max} and that these controlling factors are also correlated with each other. Quantifying N deposition's contribution to the variation in A_{max} after accounting for climate is therefore not unambiguous and requires greater attention in future studies. The cross-correlations between climate and N deposition, which are especially evident for evergreen needleleaf sites in the N limited range, prevent assessing their relative role in influencing A_{max} within the FLUXNET network. Evergreen broadleaf forests' A_{max} also show significant relationships to climate and N deposition, but a limited number of sites prevent a detailed analysis. The hypothesis cannot be confirmed for deciduous broadleaf and mixed forests, for which variation can neither be attributed to climate nor N deposition.

[40] Due to these correlations, we can only give a range of potential N deposition effects on A_{max}. The strongest observed response of A_{max} to N deposition is found for evergreen needleleaf forests for all included climates within the N limited range ($< 8\,kg\,N\,ha^{-1}\,yr^{-1}$) with a slope of $2.0 \pm 0.4\,\mu mol\ CO_2\ m^{-2}\,s^{-1}$ per $1\,kg\,N\,ha^{-1}\,yr^{-1}$. For boreal forests within the N-limited zone, we derive a slope of $1.6 \pm 0.3\,\mu mol\ CO_2\ m^{-2}\,s^{-1}$ per $1\,kg\,N\,ha^{-1}\,yr^{-1}$. The pure N deposition effect may be larger or smaller because we expect climate to explain part of the observed response; however, there is no unequivocal evidence that it is not equal to zero.

[41] The observed relationship between A_{max} and N deposition can be used to derive an estimate of the potential contribution of N deposition on C sequestration. Employing assumptions about the translation of A_{max} to annual GPP and C sequestration (detailed in Appendix C) we derive an estimate of $25 \pm 5\,kg\ C\ /\ kg\,N$, which is somewhat lower than the range of C sequestration per kg N addition of 35–65 kg C / kg N reported by *Erisman et al*. [2011]. We want to stress that this estimate corresponds to the carbon that is sequestered due to enhancements in photosynthetic capacity only and is based on very crude assumptions.

4.2. Correlation of N Deposition With Climate

[42] We are not able to extract the N deposition effect after accounting for climate interactions. This correlation between N availability and temperature is partly associated with human activity, which is higher in areas with higher temperatures, causing higher N emissions and hence deposition [*Högberg*, 2007; *Dentener et al*., 2006; *Aber et al*., 2003]. Therefore, we have sound reason to assume that this strong noncausal relationship between climate and N deposition exists in reality and is not an artifact of the FLUXNET tower locations. Observational studies might therefore be potentially unable to answer the question regarding the relative effect of climate and N deposition. The interconnection of N deposition and climate for forests in the FLUXNET database is evident across the continents, demonstrating its global relevance [*Sutton et al*., 2008; *Aber et al*., 2003]. We further hypothesize that the observed response in A_{max} cannot be attributed solely to either N deposition or climate, but rather to the simultaneous reduction of limiting factors when moving across gradients of climate and N deposition.

[43] Additionally, the variable MAT, for which the correlations with N deposition were the strongest, is a surrogate for a number of underlying processes relating to N availability, such as for instance the increase in N mineralization with increasing soil temperatures [*Melillo et al*., 2011; *Kergoat et al*., 2008; *Magnani et al*., 2007; *Hyvönen et al*., 2007]. Therefore, MAT is not an ideal descriptor of pure temperature limitations on photosynthesis. We show that the alternative temperature index, MTD, describing the mean deviation of annual temperatures from the realized optimum, is a good predictor of photosynthetic capacity for forest canopies. We expect a closer direct link to photosynthesis for MTD than MAT and especially evergreen needleleaf forests show an improved trend between A_{max} and MTD. In comparison with MAT, MTD performed better for evergreen needleleaf sites in subset 1 and 2, and explained only slightly less than MAT in subset 3 (Table 2).

4.3. Critical Loads of N Deposition

[44] Our second hypothesis states that we expect a nonlinear response of A_{max} to N deposition, which we can confirm for evergreen needleleaf forests. Across the observed N deposition rates ($0–25\,kg\,N\,ha^{-1}\,yr^{-1}$) the response of photosynthetic capacity of evergreen needleleaf forests is

indeed nonlinear, leveling off at a critical threshold of ~ 8 kg N ha^{-1} yr^{-1} in our data set. Our findings agree with the N saturation hypothesis [*Aber et al*., 2003]; however, we find no signs of a second critical threshold, i.e. a decrease in A_{max} at higher rates of N deposition. The observed critical threshold for N saturation in evergreen needleleaf forests of ~ 8 kg N ha^{-1} yr^{-1} is in line with recently proposed critical loads, derived with different approaches and indicators of N saturation; 5–10 kg N ha^{-1} yr^{-1} [*Allen*, 2007], and 15 kg N ha^{-1} yr^{-1} [*Butterbach-Bahl and Gundersen*, 2011]. It is notable that N deposition, as a nonlinear predictor, best captures the variability in A_{max} across all evergreen needleleaf forests. The second hypothesis cannot be confirmed for the other forest types as no saturating response is observed.

[45] Our results indicate that C fluxes at the canopy scale are able to capture the mechanisms related to C-N cycling, and that canopy A_{max} can serve as another indicator for N saturation. The nonlinear response to N deposition or N fertilization should be kept in mind when reporting ratios for kg of C sequestration per kg of N addition and should always be reported. In addition, the range of N deposition rates and forest or ecosystems types for which a ratio is applicable is essential information.

4.4. Deciduous Broadleaf Forests Insensitive to N Deposition

[46] Deciduous broadleaf forests show no robust relationships between A_{max} and any of the included abiotic or biotic predictors. Evergreen needleleaf forests show a stronger response to N addition than deciduous forests (Figure 2a) [see also *Liu and Greaver*, 2009; *Allen*, 2007]. Physiological differences of the two forest types can explain the different sensitivities to nitrogen fertilization, e.g., evergreen needleleaf forests have lower N stocks and uptake compared to deciduous broadleaf forests, and are adapted to low nutrient environments, resulting in a generally higher sensitivity to N addition [*Hikosaka*, 2004; *Warren and Adams*, 2004; *Allen*, 2007; *Millard and Grelet*, 2010; *Butterbach-Bahl and Gundersen*, 2011]. The nonlinear response to N fertilization has been found for both forest types, but critical loads for deciduous forests have been reported to be higher (10–20 kg N ha^{-1} yr^{-1}) [*Allen*, 2007]. Similar to deciduous broadleaf forests, A_{max} at all temperate sites, regardless of forest type, shows a lack of response to N deposition across the observed range of N deposition from 2–28 kg N ha^{-1} yr^{-1} (Figure 2b). This lack of sensitivity of temperate forests to N fertilization agrees with findings of *Nadelhoffer et al*. [1999] who found a similar minimal effect of N deposition on tree growth in northern temperate forests.

[47] We hypothesize that the absence of an N deposition effect for deciduous broadleaf forests and temperate forests in our data set may be due to the following three factors. First, the N deposition effect in these forest types is small but not absent, because the limited sample size for these forests only allows detecting a strong response to N deposition (appendix B). Second, the temperate climate zones (where most deciduous broadleaf sites are found) have been exposed to high loads of N deposition over decades and/or are naturally fertile, i.e., the additional N due to N deposition is small compared to the natural N supply [*Nave et al*., 2009; *Högberg*, 2011]. Thus, although the sites are found at variable N deposition rates, the forests are in the intermediate or N-saturated stage, which would explain the absence of a response in A_{max} along an axis of N deposition. Third, N fertilization can result in aboveground tree growth without a stimulation of photosynthesis. Shifts in C-allocation from belowground to aboveground biomass, could similarly explain the absence of an N effect on canopy A_{max} [*Talhelm et al*., 2011].

4.5. LAI and Foliar N Effect on A_{max}

[48] Our third hypothesis states that foliar N and LAI have a positive effect on photosynthetic capacity, and that they in turn are related to N deposition. Climate and N deposition have a stronger predictive power of A_{max} than foliar N and LAI for evergreen needleleaf forests. We show that the LAI and/or foliar N effect on canopy photosynthetic capacity are not stronger than the effect of temperature, precipitation, or N deposition in our data set. The foliar N concentration – A_{max} relationship is thought to be stable across a variety of conditions, and for different species of the same functional type [*Kattge et al*., 2009]. We identify a strong correlation across forest types but only a weak relationship within evergreen needleleaf forests. This confirms *Reich et al*. [1995] who stated that within species groups or for individual species, there may be markedly different A_{max}-foliar N relationships. LAI and foliar N influence canopy photosynthesis [*Kergoat et al*., 2008; *Lindroth et al*., 2008]. However, their interconnection to climate and N availability should be appreciated when assessing drivers of canopy A_{max}.

[49] We observe a significant relationship between N deposition and foliar N across forest types and within evergreen needleleaf forests. The relationship between N deposition and foliar N has been established earlier [*De Vries et al*., 2003], but has also been reported as absent [*Aber et al*., 2003]. LAI cannot be linked to N deposition for any forest type in our study. The absence of a relationship between N deposition and LAI, as well as the absence of a relationship between foliar N and N deposition in the N-limited range, cannot be taken as proof of absence of the photosynthesis enhancing mechanisms. We hypothesize that the inherent difficulties associated with LAI and foliar N measurements, and with their spatial and temporal integration are responsible [*Aber et al*., 2003; *Bréda*, 2003]. Overall our results do not provide unequivocal evidence for or against either mechanism over which N is potentially able to enhance canopy photosynthesis [*Janssens and Luyssaert*, 2009; *Gough et al*., 2004]. *Gough et al*. [2004] reported that fertilization temporarily increases leaf level photosynthesis in pine and that additional photo-assimilates were used to increase leaf area. We believe that observational studies employing an across-site approach like ours may not be able to detect changes in stand characteristics acting at varying temporal scales at the local scale.

4.6. Limitations of the Approach

[50] Our analysis includes several sources of uncertainties: the flux measurements, the modeled N deposition, and the LAI and foliar N data. The uncertainties of the modeled N deposition maps are associated with the results of the model ensemble and the large resolution employed; details can be found in *Dentener et al*. [2006]. Modeled N deposition should be regarded as an indicator of true N deposition and

modeled deposition to forests is usually underestimated [*Flechard et al*., 2010; *Erisman and Draaijers*, 2003]. Furthermore, A_{max} estimates are based on 1–8 years of data per site, which caused A_{max} to be more accurate for some sites than for others. We included managed and unmanaged forests sites, exhibiting a high degree of variability in terms of site characteristics and species. The effects of ozone or carbon dioxide on photosynthesis are not included in the analysis. Site-specific measurements of N deposition, and a standardized sampling scheme for LAI and foliar/canopy N, ensuring the representativeness of the measurements for the tower footprint and allowing an adequate assessment of their connection to canopy A_{max}, are expected to refine the presented analysis.

5. Conclusion

[51] This study shows that N deposition is nonlinearly related to canopy A_{max} in evergreen needleleaf forests with a close linear relationship in the N limited range. Deciduous broadleaf forests exhibit zero to little response to N deposition. However, close correlations between N deposition and climate and their comparable influences on canopy A_{max} prevents the separation of their effects. This calls for caution, and studies of climate effects on C cycling should account for potential N effects and vice versa. The close linkage of N deposition and climate is potentially a global phenomenon and complicates the use of observational studies for assessing drivers of carbon cycling. Overcoming these inherent linkages is essential in separating climate and N effects. Measures of N cycling and pools should be adopted as standards in the FLUXNET network, e.g., N deposition, foliar and soil N concentrations, to facilitate the mechanistic assessment of C and N cycling, their interactions and the effect of climate. Furthermore, process-based modeling studies are valuable tools to elucidate the confounding effects of climate and N deposition.

[52] The observed response of canopy A_{max} to levels of N deposition agrees with the N saturation hypothesis, demonstrating that flux tower measurements are suitable for testing hypotheses of nitrogen-photosynthesis relationships at the canopy scale. The extension of the approach to ecosystems and climate conditions underrepresented in this study, as well as the investigation of other relevant physiological processes, i.e., ecosystem respiration, are expected to substantially increase our understanding of carbon-nitrogen interactions in terrestrial ecosystems.

Appendix A: Overview of Light Response Curves

[53] The procedure for calculating A_{max} from half-hourly GPP estimates is detailed below. GPP was plotted as a function of light intensity (PPFD) and the threshold light intensity ($PPFD_{sat}$) was determined, below which GPP is limited by light. Standard values for the different climate zones were chosen. $PPFD_{sat}$ of 1200 $\mu mol\ m^{-2}\ s^{-1}$ proved suitable for most climates. However, a lower $PPFD_{sat}$ of 800 $\mu mol\ m^{-2}\ s^{-1}$ was chosen for boreal and temperate climates, and a higher level for tropical climates at $PPFD_{sat} = 1400\ \mu mol\ m^{-2}\ s^{-1}$. These are conservative estimates, in regard to the minimum PPFD of apparent light saturation. Each light response curve was checked visually and the light-saturation threshold was adjusted if necessary, to derive an A_{max} estimate that is not biased by light limiting conditions. For all GPP above $PPFD_{sat}$ A_{max} was calculated as the average of the upper 95th–98th percentile. The highest two percent of GPP data were excluded to reduce the effect of outliers. The estimates of A_{max} were not strongly influenced by minor changes of the chosen threshold.

[54] A_{max} is by definition the rate that is achieved under optimal growing conditions, i.e., when photosynthesis is not limited by water stress, suboptimal or superoptimal temperatures, stomatal closure, diseases, air pollution stress (e.g. ozone), and pests [*Field and Mooney*, 1986]. There is no guarantee that optimal growing conditions were present during the record period because, for example, Mediterranean sites can be permanently under water and/or heat stress [*van der Molen et al*., 2011]. We understand that A_{max} estimates derived from field flux measurements do not represent optimal conditions, but most optimal conditions experienced for a given time period and location. Figure A1 illustrates how A_{max} was calculated for four sites (DE-Har, IT-Ren, NL-Loo, and US-SP1).

Appendix B: Power Analysis of Sample Sizes

[55] The power of the tested A_{max}-N deposition relationships for selected forest groups was assessed by means of power analysis. Detailed descriptions of the concept of power analysis can be found in most statistical textbooks, as well as in *Cohen* [1988]. Here, the input and result are detailed for the employed function pwr() in R [*R Development Core Team*, 2011];

[56] 1. Deciduous broadleaf forests: u = numerator of degrees of freedom = 2–1 = 1, v = denominator of degrees of freedom = 19–2 = 17, α = significance level = 0.05, β = power = 0.8, $f2$ = effect size = $R^2/(1–R^2)$ = 0.32/(1–0.32) = 0.47. This shows that the sample size of 19 forests would allow detecting a response larger than an R^2 of 0.32 with 80% probability.

[57] 2. Mixed forests: u = numerator of degrees of freedom = 2–1 = 1, v = denominator of degrees of freedom = 9–2 = 7, α = significance level = 0.05, β = power = 0.8, $f2$ = effect size = $R^2/(1–R^2)$ = 0.55/(1–0.55) = 1.22. This shows that the sample size of 9 forests would allow detecting a response larger than an R^2 of 0.55 with 80% probability.

Appendix C: Calculation of C Sequestration Rates

[58] The conversion of the slope of the A_{max}-N deposition relationship to estimates of sequestered C per kg N added was made using the following assumptions and calculations. It is assumed that 1% of all C assimilates are sequestered [*Steffen et al*., 1998] and that plants generally operate at 50% of A_{max}, i.e., average GPP is near 50% of A_{max} during the growing season [*Schulze*, 2006]. To account for seasonal variation in A_{max} during the year, it is assumed that 66% of the year this relationship holds, representing an 8 months long growing season. The slope is in units of [$\mu mol\ CO_2\ m^{-2}\ s^{-1}$ per 1 kg N $ha^{-1}\ yr^{-1}$] and needed to be converted to [kg C per kg N], for which the following multipliers apply: (1) from µmol to g = 1.2 * 10^{-5}, (2) from g to kg = 1 * 10^{-3}, (3) from m^{-2} to ha^{-1} * 10^4, (4) from s^{-1} to yr^{-1} = 3.1536*10^7, (5) from A_{max} to annual GPP = 0.5*0.667, (6) from GPP to C sequestration = 1 * 10^{-2}, which amounts to a multiplier of 12.62.

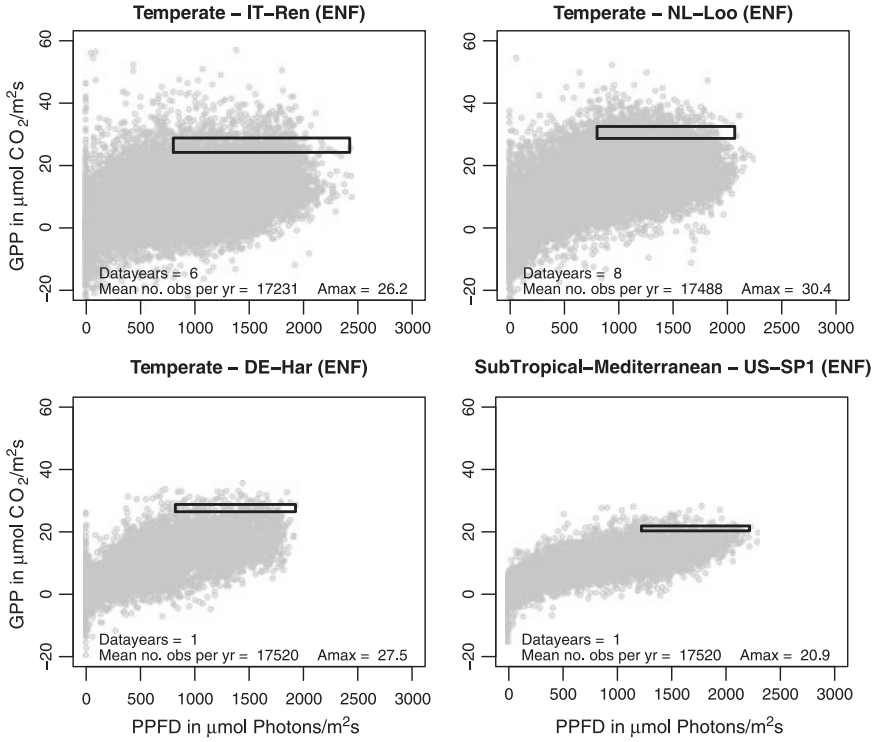

Figure A1. Light response curves with GPP (in µmol CO_2 m^{-2} s^{-1}) as a function of PPFD (in µmol photons m^{-2} s^{-1}) for four representative sites (IT-Ren, NL-Loo, DE-Har, and US-SP1).

[59] Therefore, 1 µmol CO_2 m^{-2} s^{-1} per 1 kg N ha^{-1} yr^{-1} is equivalent to ~ 13 kg C sequestered per kg N added based on the assumptions above. The percentage of C that is sequestered and annual GPP is a large uncertainty in this estimation. It is very much dependent on other processes than photosynthesis and on the region and ecosystems considered [*Piao et al*., 2009; *Luyssaert et al*., 2007; *Hyvönen et al*., 2007; *Schulze*, 2006]. However, it is a conservative (low) estimate because recent estimates state that about 1.5% is actually sequestered, which would amount to ~ 19 kg C per kg N [*Steffen et al*., 1998].

[60] **Acknowledgments**. We acknowledge NWO for providing a Ph. D. grant (NWO 829.09.006) enabling the research to be carried out by Katrin Fleischer. We thank all the scientists involved in the continuous collection of FLUXNET measurements and maintaining the data sets, which made this study possible. The eddy covariance data were acquired by the FLUXNET community and in particular by the following networks: AmeriFlux (U.S. Department of Energy, Biological and Environmental Research, Terrestrial Carbon Program (DE-FG02-04ER63917 and DE-FG02-04ER63911)), AsiaFlux, CarboEuropeIP, ChinaFlux, Fluxnet-Canada (supported by CFCAS, NSERC, BIOCAP, Environment Canada, and NRCan), LBA and OzFlux. We acknowledge the financial support to the eddy covariance data harmonization provided by CarboEuropeIP, FAO-GTOS-TCO, iLEAPS, Max Planck Institute for Biogeochemistry, National Science Foundation, University of Tuscia, Université Laval and Environment Canada and US Department of Energy and the database development and technical support from Berkeley Water Center, Lawrence Berkeley National Laboratory, Microsoft Research eScience, Oak Ridge National Laboratory, University of California - Berkeley, University of Virginia. Participation of authors from the Free University of Bozen (Italy), Virginia Commonwealth University (USA), Georg-August-University Göttingen (Germany) and the IASMA Research and Innovation centre (Italy) occurred through the FLUXNET network. Furthermore, we want to thank two anonymous reviewers.

References

Aber, J. D., K. J. Nadelhoffer, P. Steudler, and J. M. Melillo (1989), Nitrogen saturation in northern forest ecosystems, *Bioscience*, *39*, 378–386.

Aber, J., W. McDowell, K. Nadelhoffer, A. Magill, G. Berntson, M. Kamakea, S. McNulty, W. Currie, L. Rustad, and I. Fernandez (1998), Nitrogen saturation in temperate forest ecosystems - Hypotheses revisited, *Bioscience*, *48*(11), 921–934.

Aber, J., C. Goodale, S. Ollinger, M. Smith, A. Magill, M. Martin, R. Hallett, and J. Stoddard (2003), Is nitrogen deposition altering the nitrogen status of northeastern forests?, *Bioscience*, *53*(4), 375–389.

Allen, E. (2007), Effects of nitrogen deposition on forest ecosystems, in Effects of nitrogen deposition on forests and peatlands: A literature review and discussion of the potential impacts of nitrogen deposition in the Alberta oil sands region, Wood Buffalo Environmental Association.

Baldocchi, D., et al. (2001), FLUXNET: A new tool to study the temporal and spatial variability of ecosystem-scale carbon dioxide, water vapor, and energy flux densities, *Bull. Am. Meteorol. Soc.*, *82* (11), 2415–2434.

Baldocchi, D. D., K. B. Wilson, and L. Gu (2002), How the environment, canopy structure and canopy physiological functioning influence carbon, water and energy fluxes of a temperate broad-leaved deciduous forest: an assessment with the biophysical model CANOAK, *Tree Phys.*, *22*(15–16), 1065–1077, doi:10.1093/treephys/22.15-16.1065.

Bequet, R., V. Kint, M. Campioli, D. Vansteenkiste, B. Muys, and R. Ceulemans (2011), Influence of stand, site and meteorological variables on the maximum leaf area index of beech, oak and Scots pine, *Eur. J. Forest Res.*, *1–13*, doi:10.1007/s10342-011-0500-x.

Bréda, N. J. J. (2003), Ground-based measurements of leaf area index: a review of methods, instruments and current controversies, *J. Exp. Bot.*, *54*(392), 2403–2417, doi:10.1093/jxb/erg263.

Burnham, K. P., and D. R. Anderson (1998), Model Selection and Inference: A Practical Information-Theoretical Approach, Springer-Verlag, New York, NY.

Butterbach-Bahl, K., and P. Gundersen (2011), Nitrogen processes in terrestrial ecosystems, in The European Nitrogen Assessment, edited by M. Sutton et al., pp. 99–125, Cambridge University Press, Cambridge.

Canadell, J. G., C. Le Quéré, M. R. Raupach, C. B. Field, E. T. Buitenhuis, P. Ciais, T. J. Conway, N. P. Gillett, R. A. Houghton, and G. Marland (2007), Contributions to accelerating atmospheric CO2 growth from economic activity, carbon intensity, and efficiency of natural sinks, *PNAS*, *104*(47), 18866–18870, doi:10.1073/pnas.0702737104.

Churkina, G., S. Zaehle, J. Hughes, N. Viovy, Y. Chen, M. Jung, B. W. Heumann, N. Ramankutty, M. Heimann, and C. Jones (2010), Interactions between nitrogen deposition, land cover conversion, and climate change determine the contemporary carbon balance of Europe, *Biogeosci. Discuss.*, *7*(2), 2227–2265, doi:10.5194/bgd-7-2227-2010.

Ciais, P., et al. (2010), Can we reconcile atmospheric estimates of the Northern terrestrial carbon sink with land-based accounting?, *Curr. Opin. Environ. Sustain.*, *2*(4), 225–230, doi:10.1016/j.cosust.2010.06.008.

Cohen, J. (1988), Statistical power analysis for the behavioral sciences, Lawrence Erlbaum Associates, New Jersey.

Dentener, F., et al. (2006), Nitrogen and sulfur deposition on regional and global scales: A multimodel evaluation, *Global Biogeochem. Cycles*, *20*, GB4003, doi:10.1029/2005GB002672.

Desai, A. R., et al. (2008), Cross-site evaluation of eddy covariance GPP and RE decomposition techniques, *Agr. Forest Meteorol.*, *148*(6–7), 821–838, doi:10.1016/j.agrformet.2007.11.012.

Dronova, I., K. Bergen, and D. Ellsworth (2011), Forest Canopy Properties and Variation in Aboveground Net Primary Production over Upper Great Lakes Landscapes, *Ecosystems*, *14*, 865–879, doi:10.1007/s10021-011-9451-9.

Erisman, J. W., and G. Draaijers (2003), Deposition to forests in Europe: most important factors influencing dry deposition and models used for generalisation, *Environ. Pollut.*, *124*(3), 379–388, doi:10.1016/S0269-7491(03)00049-6.

Erisman, J. W., and W. de Vries (2000), Nitrogen deposition and effects on European forests, *Environ. Rev.*, *8*(2), 65–93, doi:10.1139/a00-006.

Erisman, J. W., M. A. Sutton, J. Galloway, Z. Klimont, and W. Winiwarter (2008), How a century of ammonia synthesis changed the world, *Nat. Geosci.*, *1*(10), 636–639, doi:10.1038/ngeo325.

Erisman, J. W., J. Galloway, S. Seitzinger, A. Bleeker, and K. Butterbach-Bahl (2011), Reactive nitrogen in the environment and its effect on climate change, *Curr. Opin. Environ. Sustain.*, *3*(5), 281–290, doi:10.1016/j.cosust.2011.08.012.

Field, C., and H. A. Mooney (1986), The photosynthesis-nitrogen relationship in wild plants, in On the economy of plant form and function: adaptative patterns of energy capture in plants, edited by T. J. Givnish, pp. 25–56, Cambridge University Press, Cambridge.

Flechard, C. R., et al. (2010), Dry deposition of reactive nitrogen to European ecosystems: a comparison of inferential models across the NitroEurope network, *Atmos. Chem. Phys. Discuss.*, *10*(12), 29291–29348, doi:10.5194/acpd-10-29291-2010.

Galloway, J., J. Aber, J. Erisman, S. Seitzinger, R. Howarth, E. Cowling, and B. Cosby (2003), The nitrogen cascade, *Bioscience*, *53*(4), 341–356.

Galloway, J. N., A. R. Townsend, J. W. Erisman, M. Bekunda, Z. Cai, J. R. Freney, L. A. Martinelli, S. P. Seitzinger, and M. A. Sutton (2008), Transformation of the Nitrogen Cycle: Recent Trends, Questions, and Potential Solutions, *Science*, *320*(5878), 889–892, doi:10.1126/science.1136674.

Gough, C. M., J. R. Seiler, and C. A. Maier (2004), Short-term effects of fertilization on loblolly pine (Pinus taeda L.) physiology, *Plant Cell Environ.*, *27*(7), 876–886, doi:10.1111/j.1365-3040.2004.01193.x.

Groenendijk, M., M. K. van der Molen, and A. J. Dolman (2009), Seasonal variation in ecosystem parameters derived from FLUXNET data, *Biogeosci. Discuss.*, *6*(2), 2863–2912, doi:10.5194/bgd-6-2863-2009.

Hikosaka, K. (2004), Interspecific difference in the photosynthesis-nitrogen relationship: patterns, physiological causes, and ecological importance, *J. Plant Res.*, *117*, 481–494, doi:10.1007/s10265-004-0174-2.

Hilborn, R., and M. Mangel (1997), The Ecological Detective: Confronting Models with Data, Princeton University Press.

Hyvönen, R., et al. (2007), The likely impact of elevated CO2, nitrogen deposition, increased temperature and management on carbon sequestration in temperate and boreal forest ecosystems: a literature review, *New Phytol.*, *173*(3), 463–480, doi:10.1111/j.1469-8137.2007.01967.x.

Högberg, P. (2007), Environmental science: Nitrogen impacts on forest carbon, *Nature*, *447*(7146), 781–782, doi:10.1038/447781a.

Högberg, P. (2011), What is the quantitative relation between nitrogen deposition and forest carbon sequestration?, *Global Change Biol.*, doi:10.1111/j.1365-2486.2011.02553.x.

Janssens, I. A., and S. Luyssaert (2009), Carbon cycle: Nitrogen's carbon bonus, *Nat. Geosci.*, *2*(5), 318–319, doi:10.1038/ngeo505.

Janssens, I. A., et al. (2003), Europe's Terrestrial Biosphere Absorbs 7 to 12% of European Anthropogenic CO2 Emissions, *Science*, *300*(5625), 1538–1542, doi:10.1126/science.1083592.

Jarvis, P. G. (1976), The Interpretation of the Variations in Leaf Water Potential and Stomatal Conductance Found in Canopies in the Field, *Philos. Trans. R. Soc. London, Ser. B*, *273*(927), 593–610.

Kattge, J., W. Knorr, T. Raddatz, and C. Wirth (2009), Quantifying photosynthetic capacity and its relationship to leaf nitrogen content for global-scale terrestrial biosphere models, *Global Change Biol.*, *15*(4), 976–991, doi:10.1111/j.1365-2486.2008.01744.x.

Kergoat, L., S. Lafont, A. Arneth, V. Le Dantec, and B. Saugier (2008), Nitrogen controls plant canopy light-use efficiency in temperate and boreal ecosystems, *J. Geophys. Res. Biogeosci.*, *113*(G4), G04017, doi:10.1029/2007JG000676.

Kottek, M., J. Grieser, C. Beck, B. Rudolf, and F. Rubel (2006), World Map of the Köppen-Geiger climate classification updated., *Meteorol. Z.*, *15*, 259–263, doi:10.1127/0941-2948/2006/0130.

Kravchenko, A. N., and Robertson, G. P. (2011), Whole-Profile Soil Carbon Stocks: The Danger of Assuming Too Much from Analyses of Too Little, *Soil Sci. Soc. Am. J. 75*(1), 235–240.

Le Quéré, C. (2010), Trends in the land and ocean carbon uptake, *Curr. Opin. Environ. Sustainability*, *2*(4), 219–224, doi:10.1016/j.cosust.2010.06.003.

Le Quéré, C., et al. (2009), Trends in the sources and sinks of carbon dioxide, *Nature Geosc.*, *2*(12), 831–836, doi:10.1038/ngeo689.

LeBauer, D. S., and K. K. Treseder (2008), Nitrogen limitation of net primary productivity in terrestrial ecosystems is globally distributed, *Ecology*, *89*(2), 371–379.

Lindroth, A., et al. (2008), Leaf area index is the principal scaling parameter for both gross photosynthesis and ecosystem respiration of Northern deciduous and coniferous forests, *Tellus Ser. B*, *60*(2), 129–142, doi:10.1111/j.1600-0889.2007.00330.x.

Liu, L., and T. L. Greaver (2009), A review of nitrogen enrichment effects on three biogenic GHGs: the CO2 sink may be largely offset by stimulated N2O and CH4 emission, *Ecol. Lett.*, *12*(10), 1103–1117, doi:10.1111/j.1461-0248.2009.01351.x.

Loveland, T. R., B. C. Reed, J. F. Brown, D. O. Ohlen, Z. Zhu, L. Yang, and J. W. Merchant (2000), Development of a global land cover characteristics database and IGBP DISCover from 1 km AVHRR data, *Int. J. Remote Sens.*, *21*, 1303–1330.

Luyssaert, S., et al. (2007), CO2 balance of boreal, temperate, and tropical forests derived from a global database, *Glob. Chang. Biol.*, *13*(12), 2509–2537, doi:10.1111/j.1365-2486.2007.01439.x.

Magnani, F., et al. (2007), The human footprint in the carbon cycle of temperate and boreal forests, *Nature*, *447*(7146), 849–851, doi:10.1038/nature05847.

Melillo, J. M., et al. (2011), Soil warming, carbon-nitrogen interactions, and forest carbon budgets, *PNAS*, doi:10.1073/pnas.1018189108.

Millard, P., and G. A. Grelet (2010), Nitrogen storage and remobilization by trees: ecophysiological relevance in a changing world, *Tree Phys.*, *30*(9), 1083–1095, doi:10.1093/treephys/tpq042.

van der Molen, M., et al. (2011), Drought and ecosystem carbon cycling, *Agr. Forest Meteorol.*, *151*(7), 765–773, doi:10.1016/j.agrformet.2011.01.018.

Nadelhoffer, K. J., B. A. Emmett, P. Gundersen, O. J. Kjonaas, C. J. Koopmans, P. Schleppi, A. Tietema, and R. F. Wright (1999), Nitrogen deposition makes a minor contribution to carbon sequestration in temperate forests, *Nature*, *398*(6723), 145–148, doi:10.1038/18205.

Nave, L. E., C. S. Vogel, C. M. Gough, and P. S. Curtis (2009), Contribution of atmospheric nitrogen deposition to net primary productivity in a northern hardwood forest, *Can. J. For. Res.*, *39*(6), 1108–1118, doi:10.1139/X09-038.

Ollinger, S. V., A. D. Richardson, M. E. Martin, D. Y. Hollinger, S. E. Frolking, P. B. Reich, L. C. Plourde, G. G. Katul, J. W. Munger, R. Oren, M.-L. Smith, K. T. Paw U, P. V. Bolstad, B. D. Cook, M. C. Day, T. A. Martin, R. K. Monson, and H. P. Schmid (2008), Canopy nitrogen, carbon assimilation, and albedo in temperate and boreal forests: Functional relations and potential climate feedbacks, *PNAS*, *105*(49), 19336–19341, doi:10.1073/pnas.0810021105.

Pan, Y., et al. (2011), A Large and Persistent Carbon Sink in the World's Forests, *Science*, *333*(6045), 988–993, doi:10.1126/science.1201609.

Papale, D., et al. (2006), Towards a standardized processing of Net Ecosystem Exchange measured with eddy covariance technique: algorithms and uncertainty estimation, *Biogeosc.*, *3*(4), 571–583, doi:10.5194/bg-3-571-2006.

Piao, S., P. Friedlingstein, P. Ciais, P. Peylin, B. Zhu, and M. Reichstein (2009), Footprint of temperature changes in the temperate and boreal forest carbon balance, *Geophys. Res. Lett.*, *36*(7), L07404.

Reay, D. S., F. Dentener, P. Smith, G. Grace, and R. A. Feely (2008), Global nitrogen deposition and carbon sinks, *Nat. Geosci.*, *1*(7), 430–437, doi:10.1038/ngeo230.

Reich, P. B., M. B. Walters, B. D. Kloeppel, and D. S. Ellsworth (1995), Different photosynthesis-nitrogen relations in deciduous hardwood and evergreen coniferous tree species, *Oecol.*, *104*, 24–30, doi:10.1007/BF00365558.

Reichstein, M., et al. (2005), On the separation of net ecosystem exchange into assimilation and ecosystem respiration: review and improved algorithm, *Global Change Biol.*, *11*(9), 1424–1439, doi:10.1111/j.1365-2486.2005.001002.x.

Reichstein, M., et al. (2007), Determinants of terrestrial ecosystem carbon balance inferred from European eddy covariance flux sites, *Geophys. Res. Lett.*, *34*(1), L01402, doi:10.1029/2006GL027880.

Rodgers, J. L., and W. A. Nicewander (1988), Thirteen ways to look at the correlation coefficient, *Am. Stat.*, *42*, 59–66.

R Development Core Team (2011), R: A Language and Environment for Statistical Computing, *R Foundation for Statistical Computing*, Vienna, Austria, ISBN 3-900051-07-0.

Schulze, E., E. Beck, and K. Müller-Hohenstein (2005), Plant Ecology, Springer Verlag, Heidelberg.

Schulze, E.-D. (2006), Biological control of the terrestrial carbon sink, *Biogeosc.*, *3*(2), 147–166, doi:10.5194/bg-3-147-2006.

Steffen, W., et al. (1998), The Terrestrial Carbon Cycle: Implications for the Kyoto Protocol, *Science*, *280*(5368), 1393–1394, doi:10.1126/science.280.5368.1393.

Sutton, M. A., D. Simpson, P. E. Levy, R. I. Smith, S. Reis, M. Van Oijen, and W. De Vries (2008), Uncertainties in the relationship between atmospheric nitrogen deposition and forest carbon sequestration, *Global Change Biol.*, *14*(9), 2057–2063, doi:10.1111/j.1365-2486.2008.01636.x.

Talhelm, A. F., K. S. Pregitzer, and A. J. Burton (2011), No evidence that chronic nitrogen additions increase photosynthesis in mature sugar maple forests, *Ecol. Appl.*, *21*(7), 2413–2424.

Thomas, R. Q., C. D. Canham, K. C. Weathers, and C. L. Goodale (2010), Increased tree carbon storage in response to nitrogen deposition in the US, *Nat. Geosci.*, *3*(1), 13–17.

de Vries, W., et al. (2003), Intensive monitoring of forest ecosystems in Europe: 1. Objectives, set-up and evaluation strategy, *Forest Ecol. Manag.*, *174*(1–3), 77–95, doi:10.1016/S0378-1127(02)00029-4.

de Vries, W., S. Solberg, M. Dobbertin, H. Sterba, D. Laubhahn, G. J. Reinds, G.-J. Nabuurs, P. Gundersen, and M. A. Sutton (2008), Ecologically implausible carbon response?, *Nature*, *451*(7180), E1–E3, doi:10.1038/nature06579.

de Vries, W., et al. (2009), The impact of nitrogen deposition on carbon sequestration by European forests and heathlands, *Forest Ecol. Manag.*, *258*(8), 1814–1823, doi:10.1016/j.foreco.2009.02.034.

Wang, Y. P., R. M. Law, and B. Pak (2010), A global model of carbon, nitrogen and phosphorus cycles for the terrestrial biosphere, *Biogeosc.*, *7*(7), 2261–2282, doi:10.5194/bg-7-2261-2010.

Warren, C. R., and M. A. Adams (2004), Evergreen trees do not maximize instantaneous photosynthesis, *Trends Plant Sci.*, *9*(6), 270–274, doi:10.1016/j.tplants.2004.04.004.